Computational Statistics
Project Report

20th March 2020

1 Introduction

The Markov Chain Monte Carlo (MCMC) sampling tries to investigate properties of distributions by drawing random samples. This is a sequential process, where the drawing of a random sample at any given time depends only on its immediate predecessor. In this project a variant of the MCMC algorithm from the paper [Lau and Krumscheid, 2019] is reimplemented and an attempt is made to reproduce the results of the experiments. The paper under consideration builds on the ideas of [Metropolis et al., 1953, Schmeiser, 1992, Liu et al., 2000] and [Yang et al., 2019]. The source code under MIT license for this project can be found in the GitHub repository

`github.com/rinkwitz/Adaptive_Plateau_MCMC`.

Since the simulation of Markov chains is very time-consuming, you can download already simulated MCMC runs under the link

`drive.google.com/file/d/1OzUR6-axu2M8hrUERXLregBqmXdpoS-Y/view?usp=sharing`.

2 Adaptive Component-wise Multiple-Try Metropolis Algorithm

The core algorithm of the paper [Lau and Krumscheid, 2019] consists of a MCMC algorithm which fulfills three properties. First, the algorithm suggests several suggestions

from different plateau distributions during sampling. This happens independently for all components of a sample. Lastly, plateau distributions adapt their shape depending on the frequency of the accepted sample proposals.

2.1 Plateau Proposal Distributions

The MCMC algorithm in [Lau and Krumscheid, 2019] uses *non-overlapping plateau proposal distributions* for sampling. The underlying probability density function f is a combination of the density of a uniform distribution with exponential decaying tails. Here the density f is constant around a mean value μ in the closed interval $[\mu-\delta, \mu+\delta]$ with $\delta > 0$. Outside this interval the distribution follows an exponential decay with its tail width determined by $\sigma_i > 0$, depending on whether you are on the left or right side of the interval $[\mu-\delta, \mu+\delta]$. If you define an unnormalized density function

$$\tilde{f}(y;\mu,\delta,\sigma_1,\sigma_2) = \begin{cases} \exp\left(-\frac{1}{2\sigma_1^2}[y-(\mu-\delta)]^2\right), & y < \mu-\delta \\ 1, & \mu-\delta \leq y \leq \mu+\delta \\ \exp\left(-\frac{1}{2\sigma_2^2}[y-(\mu+\delta)]^2\right), & y > \mu+\delta \end{cases}$$

and then calculate the following integral

$$\begin{aligned} C(\delta,\sigma_1,\sigma_2) &= \int_{-\infty}^{\infty} \tilde{f}(y;\mu,\delta,\sigma_1,\sigma_2)dy \\ &= \int_{-\infty}^{\mu-\delta} \exp\left(-\frac{1}{2\sigma_1^2}[y-(\mu-\delta)]^2\right)dy + \int_{\mu-\delta}^{\mu+\delta} 1dy + \int_{\mu+\delta}^{\infty} \exp\left(-\frac{1}{2\sigma_2^2}[y-(\mu+\delta)]^2\right)dy \\ &= \frac{\sqrt{2\pi\sigma_1^2}}{2} + 2\delta + \frac{\sqrt{2\pi\sigma_1^2}}{2} \end{aligned}$$

as the sums of 2 half gaussian integrals and one integral over a constant function, then the normalized probability density function is $f(y;\mu,\delta,\sigma_1,\sigma_2) = C(\delta,\sigma_1,\sigma_2)^{-1}\tilde{f}(y;\mu,\delta,\sigma_1,\sigma_2)$ [Lau and Krumscheid, 2019]. Using f you can define the plateau probability density distributions $T_{j,k}$, $j \in \{1,\ldots,M\}$ for the trial proposals of the k-th component as

$$T_{j,k}(x,y) = \begin{cases} f(y;x,\delta_1,\sigma,\sigma), & j=1 \\ \frac{1}{2}f(y;x-(2j-3)\delta-\delta_1,\delta,\sigma,\sigma) + \frac{1}{2}f(y;x+(2j-3)\delta+\delta_1,\delta,\sigma,\sigma), & j=2,\ldots M-1 \\ \frac{1}{2}f(y;x-(2M-3)\delta-\delta_1,\delta,\sigma_0,\sigma) + \frac{1}{2}f(y;x+(2M-3)\delta+\delta_1,\delta,\sigma,\sigma_1), & j=M \end{cases}$$

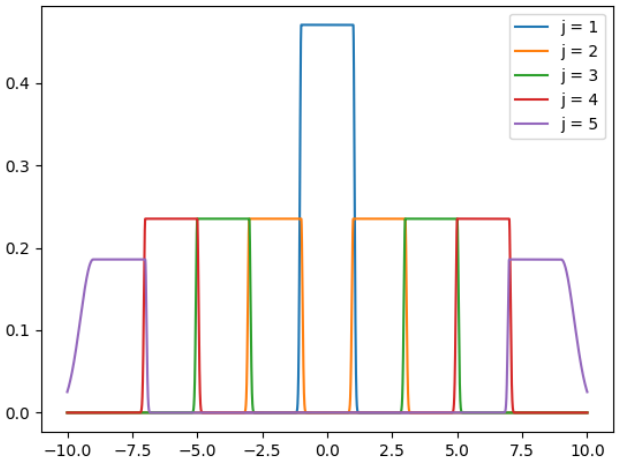

Figure 1: Trial proposal propability density distributions for $M = 5$

with values $\delta_1, \delta, \sigma, \sigma_0, \sigma_1 > 0$. In figure 1 you can see the trial proposal propability density distributions for the parameters $M = 5, \delta_1 = \delta = 1, \sigma = 0.05, \sigma_0 = \sigma_1 = 0.5$. One can see that the distributions overlap only at their exponential decaying tails. The outer tails decrease with the larger σ_0, σ_1 values shallower than the remaining tails. In the paper [Lau and Krumscheid, 2019], the authors consistently use the values $\delta = \delta_1 = 2, \sigma = 0.05, \sigma_0 = \sigma_1 = 3$.

2.2 Component-wise Multiple-Try Metropolis

The component-wise multiple-try Metropolis algorithm [Lau and Krumscheid, 2019, Algorithm 1], which forms the basis of the sampling procedure, starts from a starting position $x_0 \in \mathbb{R}^d$. For each MCMC realization x_n with $n \in \{1, \ldots, N\}$ the following procedure is used for each one of the d components. If $x = (x_1, \ldots, x_d)$ is the last sampled candidate of the MCMC algorithm, then the algorithm proposes trials z_j for $i = 1, \ldots, M$ by sampling it from the distributions $T_{j,k}(x_k, \cdot)$. In my reimplementation I use a rejection sampling procedure [Peng, 2018]. For this purpose I use an uniform

distribution to generate the samples over the following intervals

$$I_j = \begin{cases} [x_k - \delta_1 - t_1, x_k + \delta_1 + t_1] \\ \text{for } j = 1 \text{ with } t_1 = \sqrt{-2\sigma^2 \log(0.0001 C(\delta_1, \sigma, \sigma))}, \\ [x_k - 2(j+1)\delta - \delta_1 - t_2, x - 2j\delta - \delta_1 + t_2] \cup [x_k + 2j\delta + \delta_1 - t_2, x + 2(j+1)\delta - \delta_1 + t_2] \\ \text{for } j = 2, \ldots, M-1 \text{ with } t_2 = \sqrt{-2\sigma^2 \log(0.0002 C(\delta, \sigma, \sigma))}, \text{ or} \\ [x_k - 2(M+1)\delta - \delta_1 - t_{32}, x_k - 2M\delta - \delta_1 + t_{31}] \cup [x_k + 2M\delta + \delta_1 - t_{31}, x_k + 2(M+1)\delta + \delta_1 + t_{32}] \\ \text{for } j = M \text{ with } t_{31} = \sqrt{-2\sigma^2 \log(0.0002 C(\delta, \sigma, \sigma_0))}, t_{32} = \sqrt{-2\sigma_0^2 \log(0.0002 C(\delta, \sigma, \sigma_0))}. \end{cases}$$

These intervals enable effective sampling in the range of $T_{j,k}(x_k, \cdot)$ where the probability density function is greater than 0.0001. To do this, one samples a $u \sim U(0,1)$ and a $y \sim U(I_i)$ until

$$u < \frac{T_{j,k}(x_k, y)}{c|I_i|}$$

is fulfilled where $|I_j|$ is the width of the used interval I_j, g_j is the probability density function of the uniform distribution over I_j and c_j has the following values situation dependent

- $j = 1: \quad c_1 = \sup_{y \in I_1} \frac{T_{1,k}(x_k, y)}{g_1(y)} = \frac{|I_1|}{C(\delta_1, \sigma, \sigma)}$,
- $j = 2: \quad c_j = \sup_{y \in I_j} \frac{T_{j,k}(x_k, y)}{g_j(y)} = \frac{|I_j|}{2C(\delta, \sigma, \sigma)}$, and
- $j = M: \quad c_M = \sup_{y \in I_M} \frac{T_{M,k}(x_k, y)}{g_M(y)} = \frac{|I_M|}{2C(\delta, \sigma, \sigma_0)}$.

Afterwards the weights associated with the trials are

$$w_{j,k} = \pi((z_j; x_{[-k]}))T_{j,k}(x_k, z_j)\lambda_{j,k}(x_k, z_j), \quad \text{for } j = 1, \ldots, M$$

are calculated whereby $(z; x_{[-i]}) \in \mathbb{R}^d$ denotes the vector, which is identical to x in all entries except the i-th one where it takes on the value z. In addition, the non-negative and symmetric function

$$\lambda_{j,k}(x, y) = |y - x|^{2.5}$$

is used. Here the authors of [Lau and Krumscheid, 2019] refer to the results of [Yang et al., 2019]. Thus, suggestions $(z_j; x_{[-k]})$ have a high weight, which have a high probability with regard to the target distribution π, whose new proposal z_j for the k-th component regarding $T_{j,k}(x_k, \cdot)$ is very likely and where the distance function $\lambda_{j,k}$ is far enough away from x_k. Proportionally to the weights $w_{1,k}, \ldots, w_{M,k}$ a $y \in \{z_1, \ldots, z_M\}$ is then randomly drawn and for $j = 1, \ldots, M-1$ the algorithm samples $x_j^* \sim T_{j,k}(y, \cdot)$. Finally one calculates

$$\alpha = \min\left\{1, \frac{w_{1,k}(z_1, x) + \cdots + w_{M,k}(z_M, x)}{w_{1,k}(x_1^*, (y; x_{[-k]})) + \cdots + w_{M-1,k}(x_{M-1}^*, (y; x_{[-k]})) + w_{M,k}(x_k, (y; x_{[-k]}))}\right\}$$

and with that probability α the algorithm accepts the new proposal and sets $x_n = (y; x_{[-k]})$. Otherwise the algorithm keeps the old proposal and sets $x_n = x$.

2.3 Adaption of Proposal Distributions

In [Lau and Krumscheid, 2019] it is proposed to adapt the widths δ and δ_0 of the plateau distributions. In my implementation every L iterations it measures how high the number of selected suggestions $c_{j,k}$ from the plateau distributions $T_{j,k}$ are in this interval. If the middle plateau distribution is called much more than the average, that is $c_{j,k} > L\eta_1$ with $\eta_1 \in (0, 1)$, then the algorithm assumes that the plateaus are too wide and halves δ and δ_1 accordingly for the following iterations. If, on the other hand, the outermost plateau distributions are selected much more than the average, in especially $c_{M,k} > \eta_2 L$ with $\eta_2 \in (0, 1)$, then the algorithm assumes that the plateaus are too small and doubles δ and δ_1. The adaptations only take place with a constantly decreasing probability of $\max(0.99^{n-1}, 1/\sqrt{n})$. This implementation of the adaptation procedure is based on [Lau and Krumscheid, 2019, Algorithm 2].

3 Experiments and Results

3.1 Performance Measures

3.1.1 Integrated Autocorrelation Times

The authors in the paper [Lau and Krumscheid, 2019] use two performance measures to assess the effectiveness of the implemented algorithm. One of these is the integrated autocorrelation times (ACT), which is measured in R MCMC simulations with N steps for K components. Let in the following be $X_t^{(r)} = (X_{t,1}^{(r)}, \ldots, X_{t,K}^{(r)})$ the result of the r-th

MCMC simulation at step t, where $r \in \{1, \ldots, R\}$ and $t \in \{1, \ldots, N\}$. First of all, one estimates the normalized autocorrelation $\hat{p}_{\tau,k}^{(r)}$ by means of

$$\hat{c}_{\tau,k}^{(r)} = \frac{1}{N-\tau} \sum_{i=1}^{N-\tau} (X_{i,k}^{(r)} - \bar{X_k}^{(r)})(X_{i+\tau,k}^{(r)} - \bar{X_k}^{(r)}) \text{ and}$$

$$\hat{p}_{\tau,k}^{(r)} = \frac{\hat{c}_{\tau,k}^{(r)}}{\hat{c}_{0,k}^{(r)}}$$

where $\bar{X_k}^{(r)} = 1/N \sum_{i=1}^{N} X_{i,k}^{(r)}$ is the arithmetic mean of the k-th component in the r-th simulation. Afterwards one approximates the integrated autocorrelation times as

$$\hat{\tau}_k^{(r)} = 1 + 2 \sum_{\tau=1}^{M} \hat{p}_{\tau,k}^{(r)}$$

[Foreman-Mackey, 2020] where $M \ll N$. To determine M the implementation uses a *initial monotone sequence estimator* as introduced by [Schmeiser, 1992]. where M is the largest natural number, so that $\hat{p}_{\tau,k}^{(r)} > 0$ applies to all $\tau \in \{1, \ldots, 2M+1\}$ and and the subsequence $(\hat{p}_{2\tau,k}^{(r)} + \hat{p}_{2\tau+1,k}^{(r)})_{\tau=1,\ldots,M}$ is monotone [Schmeiser, 1992].

3.1.2 Average Squared Jump Distance

Another performance measure is the average squared jump distance (ASJD)

$$\text{ASDJ}_k^{(r)} = \frac{1}{N} \sum_{i=1}^{N} |X_{i,k}^{(r)} - X_{i-1,k}^{(r)}|^2$$

for the k-th component and the r-th repetition of the Markov chain [Lau and Krumscheid, 2019]. Larger ASJD values are preferred, as they indicate that the state-space is better explored [Lau and Krumscheid, 2019].

3.2 Experiments

3.2.1 Target Distributions

As experiments to test the performance of the adaptive plateau-based MCMC method [Lau and Krumscheid, 2019] examines four target distributions with the Markov chain. The target distributions are

- π_1 : a mixture of 4-dimensional Gaussians $\frac{1}{2}\mathcal{N}(\mu_1, \Sigma_1) + \frac{1}{2}\mathcal{N}(\mu_2, \Sigma_2)$ with $\mu_1 = (5, 5, 0, 0)^T, \mu_2 = (15, 15, 0, 0)^T, \Sigma_1 = \text{diag}(6.25, 6.25, 6.25, 0.01), \Sigma_2 = \text{diag}(6.25, 6.25, 0.25, 0.01)$,
- π_2 : an 8-dimensional banana distribution with density $f \circ \phi$, where f is the density of an 8-dimensional normal distribution $\mathcal{N}(0, \Sigma_3)$ with $\Sigma_3 = \text{diag}(100, 1, \ldots, 1)$ and $\phi(x) = (x_1, x_2 + 0.03x_1^2 - 3, x_3, \ldots, x_8)$ for $x \in \mathbb{R}^8$,
- π_3 : a perturbed 2-dimensional gaussian with unnormalized probability density $\tilde{\pi_3}(x) = \exp\left(-x^T A x - \cos\left(\frac{x_1}{0.1}\right) - 0.5\cos\left(\frac{x_2}{0.1}\right)\right)$ for $x \in \mathbb{R}^2$ with $A = \begin{pmatrix} 1 & 1 \\ 1 & 3/2 \end{pmatrix}$, and
- π_4 : a 1-dimensional bi-stable distribution with unnormalized distribution $\tilde{\pi_4}(x) = \exp\left(-x^4 + 5x^2 - \cos\left(\frac{x}{0.02}\right)\right)$ for $x \in \mathbb{R}$.

These distributions are shown in Figure 2, which is based on [Lau and Krumscheid, 2019, Figure 3]. The representation of π_2 in Figure 2b results from a dimensionally reduced simplification, since a marginal with 6 integration variables was computationally too expensive. One can also recognize this by the fact that the probability density here is greater than that in [Lau and Krumscheid, 2019].

3.2.2 Simulation Parameter Settings

For each of the 4 target distributions $R = 200$ MCMC simulations are performed with $N = 4000$ iterations for π_1, $N = 10000$ iterations for π_2, and $N = 3000$ iterations for π_3 and π_4. The remaining parameters are the same for all simulations. These are

- $M = 5$ different plateau proposal distributions,
- $\delta = \delta_1 = 2$ widths of plateaus,
- $\sigma = 0.05$ and $\sigma_0 = \sigma_1 = 3$ flatness of the plateau tails,
- $\eta_1 = \eta_2 = 0.4$ minimum amount for an adaptation to occur,
- $L = 40$ length of the interval between adaptations, and
- a burn-in portion of 0.5 of all iterations.

These parameters are set exactly as in [Lau and Krumscheid, 2019] except L, for which there is no exact specification.

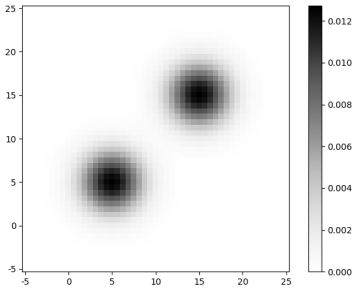

(a) Joint PDF of components 1 and 2 of π_1

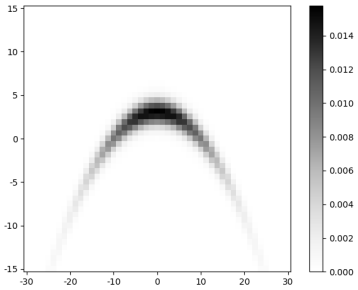

(b) Joint PDF of components 1 and 2 of π_2

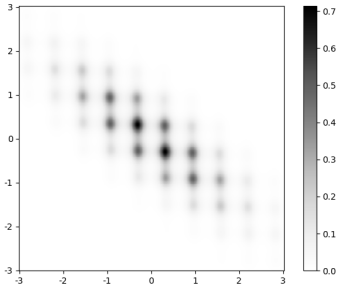

(c) PDF of π_3

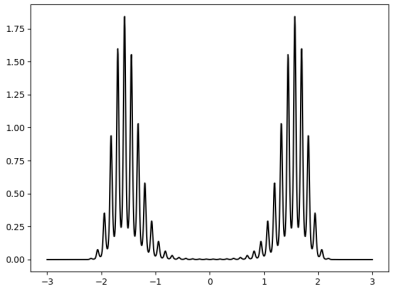

(d) PDF of π_4

Figure 2: Overview of target distributions

3.3 Results

The violin plots belonging to the experiments can be found for the target distributions π_1, π_2, π_3 and π_4 in the figures 3, 4, 5 and 6. One finds the component-wise representation of the ACT distribution in the subfigures 3a, 4a, 5a and 3a, and the component-wise representation of the ASJD distribution in the subfigures 3b, 4b, 5b and 6b. In order to better estimate the results, the tables 1, 2 and 3 contain the median, mean, minimum and maximum in rounded form listed for ACT, log-ACT and ASJD results of the experiments.

	π_1	π_2
median	8.999, 9.149, 5.126, 12.131	82.767, 88.027, 3.179, 3.17, 3.173, 3.168, 3.17, 3.181
mean	9.117, 9.171, 5.019, 14.828	92.596, 102.911, 3.168, 3.159, 3.164, 3.156, 3.165, 3.167
min	7.594, 7.277, 3.247, 3.042	54.33, 46.736, 3.022, 3.007, 3.019, 3.034, 3.032, 3.03
max	11.145, 11.295, 6.262, 102.043	231.547, 246.187, 3.354, 3.318, 3.325, 3.323, 3.347, 3.354
	π_3	π_4
median	7.769, 8.155	3.62
mean	7.821, 8.288	3.635
min	6.569, 6.84	3.337
max	9.722, 10.042	4.36

Table 1: Rounded statistical results of ACT component-wise

	π_1	π_2
median	2.197, 2.214, 1.634, 2.496	4.416, 4.478, 1.157, 1.154, 1.155, 1.153, 1.154, 1.157
mean	2.207, 2.213, 1.605, 2.382	4.488, 4.551, 1.153, 1.15, 1.152, 1.149, 1.152, 1.152
min	2.027, 1.985, 1.178, 1.113	3.995, 3.845, 1.106, 1.101, 1.105, 1.11, 1.109, 1.108
max	2.411, 2.424, 1.835, 4.625	5.445, 5.506, 1.21, 1.199, 1.202, 1.201, 1.208, 1.21
	π_3	π_4
median	2.05, 2.099	1.286
mean	2.053, 2.111	1.289
min	1.882, 1.923	1.205
max	2.274, 2.307	1.473

Table 2: Rounded statistical results of log-ACT component-wise

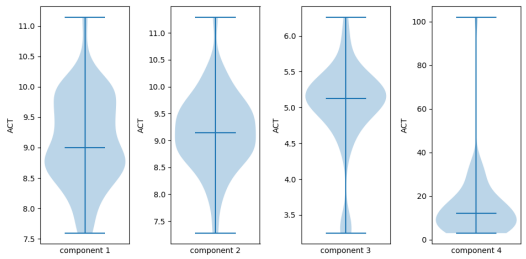

(a) Component-wise ACT distributions for target distribution π_1

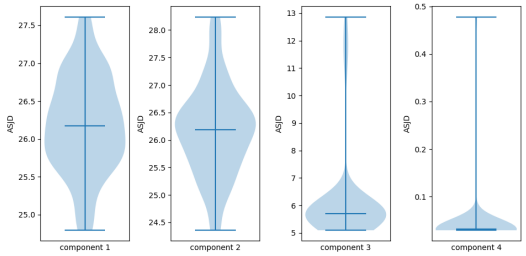

(b) Component-wise ASJD distributions for target distribution π_1

Figure 3: Violin plots of performance measures for target distribution π_1

	π_1	π_2
median	26.172, 26.186, 5.691, 0.032	9.508, 2.907, 2.948, 2.945, 2.942, 2.938, 2.953, 2.952
mean	26.191, 26.169, 6.158, 0.041	9.791, 2.922, 2.972, 2.965, 2.949, 2.96, 3.033, 2.977
min	24.792, 24.357, 5.095, 0.029	8.315, 2.837, 2.852, 2.858, 2.854, 2.841, 2.863, 2.86
max	27.612, 28.239, 12.865, 0.478	21.963, 3.306, 3.698, 3.522, 3.161, 3.534, 3.651, 3.648
	π_3	π_4
median	1.641, 0.894	3.527
mean	1.65, 0.905	3.514
min	1.512, 0.856	2.641
max	1.779, 1.166	3.736

Table 3: Rounded statistical results of ASJD component-wise

4 Discussion

The results partly differ significantly from those of the simulations in [Lau and Krumscheid, 2019]. However, the ratios of the order of magnitude between the components of the ACT and

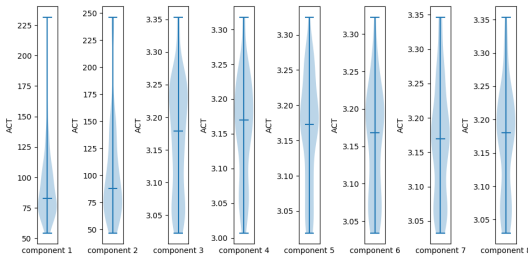

(a) Component-wise ACT distributions for target distribution π_2

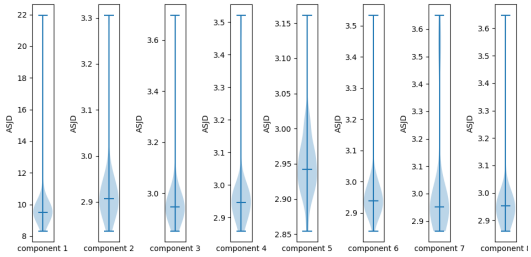

(b) Component-wise ASJD distributions for target distribution π_2

Figure 4: Violin plots of performance measures for target distribution π_2

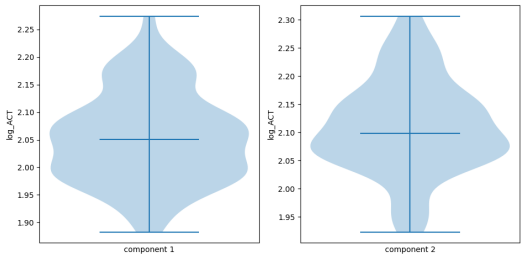

(a) Component-wise ACT distributions for target distribution π_3

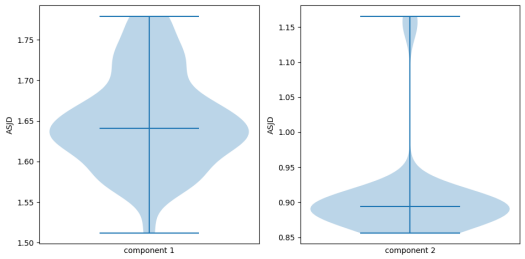

(b) Component-wise ASJD distributions for target distribution π_3

Figure 5: Violin plots of performance measures for target distribution π_3

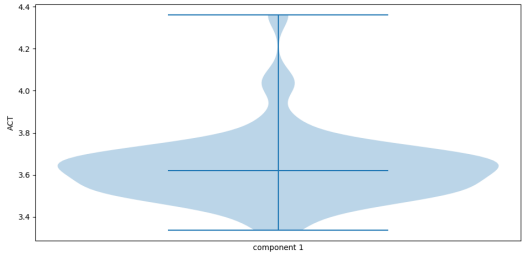

(a) ACT distribution for target distribution π_4

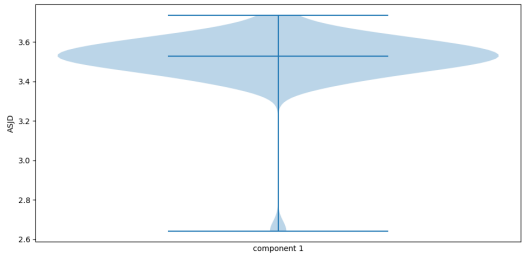

(b) ASJD distribution for target distribution π_4

Figure 6: Violin plots of performance measures for target distribution π_4

ASJD values appear to be largely consistent. In the ACT distributions, there is a close similarity between [Lau and Krumscheid, 2019] and this reimplementation (Tables 1 and 2) in the target distributions π_2 and π_4, but large deviations for π_1 and π_3. There is also a high similarity in the ASJD distributions for the target distributions π_2 and π_4 between [Lau and Krumscheid, 2019] and this project (Table 3). For the target distributions π_1 and π_3 we can observe differences in the values, but the ratios between the components are very similar to the ones in [Lau and Krumscheid, 2019]. Additionally I had the subjective impression that there were big variances in the ACT and ASJD distributions in experiments for the target distribution π_4. Unfortunately I could not compare to the MCMC algorithms MH, AG1 and AG2 [Lau and Krumscheid, 2019] due to time constraints. Therefore the higher effectiveness of the adaptive plateau-based multiple-try MCMC algorithm, which the authors have concluded in [Lau and Krumscheid, 2019], can I neither confirm nor dispute.

5 Technical Details of Implementation

The reimplementation of [Lau and Krumscheid, 2019] is written in Python 3 and uses the packages `Numpy`, `Scipy` and `Matplotlib`. The four simulations for reproducing the

MCMC results can be started with the script `run_simulations.py`, which runs all four simulations in parallel using `multiprocessing`. The adjustable parameters can be found under `adjustable parameters` in the script. They follow the naming convention from this report and the paper [Lau and Krumscheid, 2019]. After the simulations have been run, the script `create_violin_plots.py` can be used to create the the violin plots for the results. Furthermore there are two scripts `create_fig_2b.py` and `create_fig_3.py` with which reproductions of the Figures 2b and 3 from [Lau and Krumscheid, 2019] can be produced. If you want to use the MCMC runs already provided in the cloud, one has to copy the extracted `Numpy`-arrays into the folder `simulations`.

References

[Foreman-Mackey, 2020] Foreman-Mackey, D. (2020). Autocorrelation time estimation by dan foreman-mackey. https://dfm.io/posts/autocorr/. Accessed: 2020-03-20.

[Lau and Krumscheid, 2019] Lau, F. D.-H. and Krumscheid, S. (2019). Plateau proposal distributions for adaptive component-wise multiple-try metropolis.

[Liu et al., 2000] Liu, J., Liang, F., and Wong, W. (2000). The multiple-try method and local optimization in metropolis sampling. *Journal of The American Statistical Association - J AMER STATIST ASSN*, 95:121–134.

[Metropolis et al., 1953] Metropolis, Nicholas, W., A., Rosenbluth, N., M., H., A., Teller, and Edward (1953). Equation of state calculations for fast computing machines. *Journal of Chemical Physics 6*, 21:1087–.

[Peng, 2018] Peng, R. D. (2018). Advanced statistical computing. https://bookdown.org/rdpeng/advstatcomp/rejection-sampling.html. Accessed: 2020-03-17.

[Schmeiser, 1992] Schmeiser, B. (1992). Practical markov chain monte carlo. *Statistical Science*, 7.

[Yang et al., 2019] Yang, J., Levi, E., Craiu, R. V., and Rosenthal, J. S. (2019). Adaptive component-wise multiple-try metropolis sampling. *Journal of Computational and Graphical Statistics*, 28(2):276–289.